The Achievable Capacity Scaling Laws of 3D Cognitive Radio Networks

Zhiqing Wei, Zhiyong Feng, Xin Yuan, Xinyu Feng, Qixun Zhang
Wireless Technology Innovation Institute
Beijing University of Posts and Telecommunications
Beijing 100876, P. R. China
Email: {weizhiqing, fengzy, yuanxin, xyfeng, zhangqixun}@bupt.edu.cn

Xin Wang
Department of Electrical and Computer Engineering
Stony Brook University
Stony Brook, NY 11794-2350
Email: xwang@ece.sunysb.edu

***Abstract*—The exploitation of spectrum opportunities in the dimension of height will bring another transmission degree of freedom for wireless networks. Besides, the modern wireless networks are deployed in the three dimensional (3D) space, which need cognitive radio technologies to enhance their performances. With these motivations, the capacity of 3D cognitive radio networks (CRNs) is addressed in this paper. Since there is one additional dimension of interference in 3D CRNs, the network protocols need to be designed to coordinate the interference and guarantee the connectivity of CRNs. Then the link capacity and routing density of 3D CRNs are investigated. Finally, we have derived the per-node capacity of primary network and secondary network respectively. We have verified that the path loss factor α has an impact on the capacity of 3D CRNs, namely, $\alpha = 3$ is a watershed of capacity scaling laws. Besides, when $\alpha > 2.5$, the capacity of 3D CRNs is higher than 2D CRNs with the same amount of nodes asymptotically. Therefore our results may provide an insight into the design of 3D cognitive radio networks.**

***Index Terms*—3D Cognitive Radio Networks; Capacity Scaling Laws; Height Dimension**

I. Introduction

Nowadays, the capacity demand and great heterogeneity of wireless networks require the flexible and comprehensive use of spectrum. Thus cognitive radio (CR) is proposed as one of the most promising technologies for efficient spectrum utilization by exploiting spectrum holes [1]. In [2], the spectrum holes in the dimensions of frequency, time, geographical space, code, angle etc. have been extensively investigated. However, the spectrum holes in the dimension of height are rarely studied. Since the exploitation of the dimension of height can bring another transmission degree of freedom, which forms three dimensional (3D) cognitive radio networks (CRNs), the capacity of CRNs can be further improved.

Meanwhile, with the innovations such as unmanned aerial vehicle (e.g., quadcopter drone), Google loon and aeronautical telecommunication, etc., the wireless networks will be widely deployed in a 3D space in the near future. Besides, in modern battlefields, 3D wireless networks need to be deployed to connect various military units together, like aircrafts, troops, and fleets [3]. Notice that in 3D wireless networks, cognitive radio technologies can also be introduced to enhance the network performance. Thus with these motivations, we study the capacity of 3D CRNs in this paper.

The capacity of large scale wireless networks has been widely explored since the seminal work of Gupta and Kumar [4]. With n ad hoc nodes randomly distributed in a two dimensional (2D) unit area, they showed that the per-node capacity is $\Theta(\frac{1}{\sqrt{n \log n}})$. They further studied the transport capacity of 3D arbitrary and random ad hoc networks in [5]. Hu *et al.* in [6] explored the capacity of 3D networks via percolation. Li *et al.* in [3] and Bai *et al.* in [7] investigated the capacity of 3D inhomogeneous ad hoc by employing a generalized physical model. As to the capacity of CRNs, Jeon *et al.* in [8] showed that in a heterogeneous environment with n secondary users and m primary users (PUs), the secondary network can achieve per-node throughput of $\Theta(\frac{1}{\sqrt{n \log n}})$. They further extended their work to a general coding model without any specific physical layer coding assumptions in [9]. Yin *et al.* in [10] achieved the same results with [8] using a more practical assumption that secondary users (SUs) only know the locations of primary transmitter. Wang *et al.* in [11] studied the capacity scaling laws of cognitive ad hoc networks over general primary network models, where primary network is a hybrid network consisting of an ad hoc network and a base station-based network. And they addressed the multicast capacity scaling laws of cognitive radio networks in [12]. However, as far as we know, there are no literatures addressing the capacity scaling laws of 3D CRNs.

In this paper, the achievable capacity of 3D CRNs is analyzed. In 3D wireless networks, since the distribution of interference sources has one additional dimension, the interference in 3D wireless networks is more severe than that in 2D wireless networks. Therefore interference coordination needs to be considered in the network protocols. We have verified that with appropriate design of network protocols, the secondary network can achieve the same capacity scaling laws as a standalone network. Besides, the path loss factor α has an impact on the capacity scaling laws of 3D CRNs, namely, $\alpha = 3$ is a watershed of capacity scaling laws. Moreover, when $\alpha \leq 2.5$, the capacity of 3D CRNs is not superior to 2D CRNs with the same amount of nodes. However, when $\alpha > 2.5$, the capacity of 3D CRNs is higher than 2D CRNs asymptotically.

The rest of this paper is organized as follows. In Section II, the system model is presented. The network protocols of PUs and SUs are designed in Section III. In Section IV, the capacity

978-1-4799-6664-6/16/$31.00 ©2016 IEEE

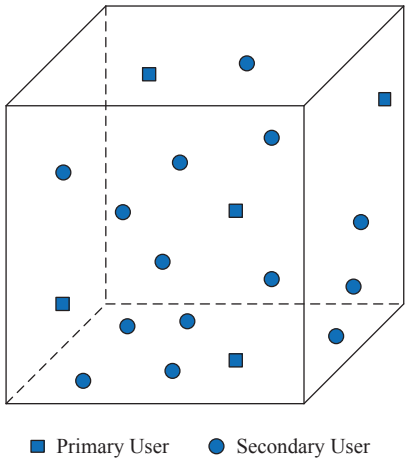

Fig. 1. The three dimensional deployment of cognitive radio networks.

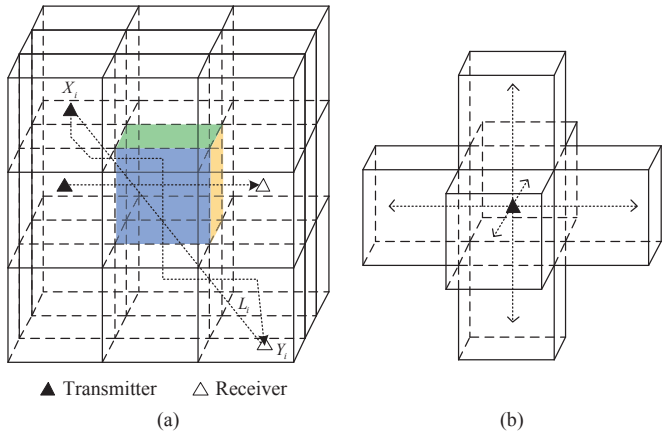

Fig. 2. (a): The routings in 3D space, (b): The data in a cube can be transmitted to 6 adjacent cubes.

scaling laws of primary network and secondary network are derived. And we summarize this paper in Section V.

II. System Model

As illustrated in Fig. 1, m PUs and n SUs are uniformly distributed in an unit cube, which share the same space and spectrum. The PUs act as if the SUs do not exist while the SUs must mitigate the interference to PUs. We assume that $n = m^{\beta}$, where $\beta > 0$. Each node has a destination, which is randomly chosen as follows. For node X, a position is uniformly picked within the unit cube, then the node nearest to it is chosen as node X's destination. The channel power gain is $g(r) = \frac{1}{r^{\alpha}}$, where r is the distance between transmitter (TX) and receiver (RX), and $\alpha > 2$ is the path loss factor.

The capacity of the ith primary TX-RX pair is

$$R_p(i) = \log\left(1 + \frac{P_p(i)g\left(\|X_{p,tx}(i) - X_{p,rx}(i)\|\right)}{N_0 + I_p(i) + I_{sp}(i)}\right) \quad (1)$$

where $P_p(i)$ is the transmit power of the ith primary TX, $X_{p,tx}(i)$ and $X_{p,rx}(i)$ are the positions of the ith primary TX and RX, respectively. $I_p(i)$ is the aggregate interference received by the ith primary RX from the primary network, while $I_{sp}(i)$ is the aggregate interference from the secondary network to the ith primary RX. N_0 is the power spectral density of the additive white Gaussian noise (AWGN). In this paper, we normalize the bandwidth to 1. The data rate of the jth secondary TX-RX pair is

$$R_s(j) = \log\left(1 + \frac{P_s(j)g\left(\|X_{s,tx} - X_{s,rx}\|\right)}{N_0 + I_s(j) + I_{ps}(j)}\right) \quad (2)$$

where $P_s(j)$ is the transmit power of the jth secondary TX, $X_{s,tx}(j)$ and $X_{s,rx}(j)$ are the positions of the jth secondary TX and RX, respectively. $I_s(j)$ is the aggregate interference received by jth secondary RX within the secondary network, $I_{ps}(j)$ is the aggregate interference from the primary network to the jth secondary RX. We denote the per-node throughput of PU and SU as $\lambda_p(m)$ and $\lambda_s(n)$, respectively [10].

III. Network Protocols

In this section, the network protocols of PUs and SUs are designed to guarantee the operations of primary and secondary networks. Firstly we do not distinguish primary network and secondary network, and denote the number of a network as k. Note that $k = m$ if this network is primary network and $k = n$ if this network is secondary network. Divide the unit cube into cubes with edge length $s_k = \left(\frac{c_0 \log k}{k}\right)^{1/3}$, where $c_0 > 0$. When a node is source node, it randomly selects a node as its destination. As illustrated in Fig. 2(a), the line segment L_i connects source X_i and destination Y_i. The packets of X_i are transmitted to Y_i in a multi-hop manner from cube to cube in the order that they are intersected by L_i, which is denoted as " straight-line routing" [14]. The transmission range of each hop is $2\sqrt{3}s_k$. Then we have the following lemma.

Lemma 1. *For the network with k nodes, denote the number of nodes that fall in a cube as N, which is a random variable. Then with high probability (w.h.p.), we have*

$$c_0\left(\frac{1}{2} - \frac{1}{e}\right)\log k \le N \le c_0 e \log k \quad (3)$$

Proof: For a specific cube, the event that node $i \in \{1, 2, ..., k\}$ falls in this cube is a Bernoulli event with probability $p_k = \frac{c_0 \log k}{k}$. Denote the number of nodes in this cube as N, then N is a random variable following Bernoulli distribution with parameters (p_k, k). We use Chernoff bound to derive the upper bound of N as follows.

$$\begin{aligned}\Pr\{N \le a\} &\le \min_{t<0} \frac{E\left[e^{tN}\right]}{e^{ta}} \\ &\overset{(a)}{=} \min_{t<0} \frac{\left(1 + (e^t - 1)p_k\right)^k}{e^{ta}} \\ &\overset{(b)}{\le} \frac{\left(1 + (e^{-\phi} - 1)p_k\right)^k}{e^{-\phi a}} \\ &\overset{(c)}{\le} \frac{k^{c_0(e^{-\phi}-1)}}{e^{-\phi a}}\end{aligned} \quad (4)$$

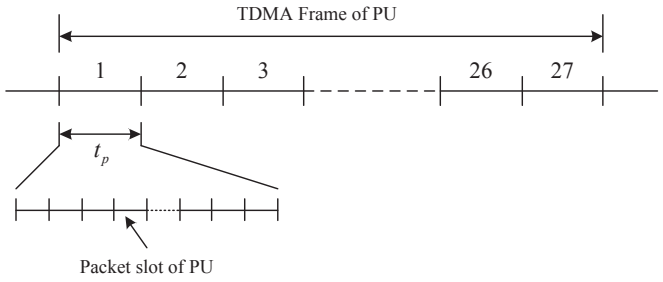

Fig. 3. The frame format of PU, which is an modification of Fig. 3 in [10].

where (a) is derived by substituting the value of $E[e^{tN}]$, (b) is derived by replacing t with a negative number $-\phi$, where $\phi > 0$. According to the inequality $1 + x \leq e^x$, we have $\left(1 + (e^{-\phi} - 1)p_k\right)^k \leq k^{9c_0(e^{-\phi}-1)}$ and (c) is achieved. Substitute $\phi = 1$ and $a = c_0\left(\frac{1}{2} - \frac{1}{e}\right)\log k$ into (4), we have

$$\Pr\{N \leq a\} \leq \frac{k^{c_0(e^{-\phi}-1)}}{e^{-\phi a}} = k^{-\frac{c_0}{2}} \tag{5}$$

When $k \to \infty$, $\Pr\left\{N \leq c_0\left(\frac{1}{2} - \frac{1}{e}\right)\log k\right\} \to 0$, therefore $N \geq c_0\left(\frac{1}{2} - \frac{1}{e}\right)\log k$ is satisfied with high probability. To find the lower bound of N, we use the Chernoff bound.

$$\begin{aligned}\Pr\{N \geq b\} &\leq \min_{t>0} \frac{E\left[e^{tN}\right]}{e^{tb}} \\ &= \min_{t>0} \frac{\left(1 + (e^t - 1)p_k\right)^k}{e^{tb}} \\ &\leq \frac{\left(1 + (e^{\phi} - 1)p_k\right)^k}{e^{\phi b}} \\ &\leq \frac{k^{c_0(e^{\phi}-1)}}{e^{\phi b}}\end{aligned} \tag{6}$$

Substitute $\phi = 1$ and $b = c_0 e \log k$ into (6), we have

$$\Pr\left\{N \geq c_0 e \log k\right\} \leq \frac{1}{k^{c_0}} \tag{7}$$

When $k \to \infty$, $\Pr\left\{N \geq c_0 e \log k\right\} \to 0$. Therefore $N \geq c_0 e \log k$ is satisfied with high probability. ■

For primary network, the cube is defined as "primary cube", whose edge is of length $s_m = \left(\frac{c_0 \log m}{m}\right)^{1/3}$ such that the connectivity of primary routings can be guaranteed. Similarly, for the secondary network, the cube is defined as "secondary cube", whose edge is of length $s_n = \left(\frac{c_0 \log n}{n}\right)^{1/3}$ to guarantee the connectivity of secondary routings. With the premise of Lemma 1, the network protocols of PUs and SUs can be designed, which mainly refer to [10].

A. Network protocols of PUs

1) The primary cubes form clusters. Each primary cluster has 27 primary cubes. Therefore primary network adopts 27-TDMA transmission protocol. As illustrated in Fig. 3, each frame of PU consists of 27 primary time slots. Each primary time slot with time length t_p is allocated to one primary cube for data transmission. In one cluster, each primary cube transmits data in a round-robin manner.
2) The data of PU is transmitted from the source to destination following the straight-line routing as illustrated in Fig. 2(a). As illustrated in Fig. 2(b), the packets can be transmitted to one of the 6 adjacent cubes.
3) When a primary cube is active, it divides its time slot into multiple packet slots. Each routing passing through or originating at the primary cube uses one of the packet slots to transmit data, as illustrated in Fig. 3.
4) The transmit power of PU is $P_0 s_m^{\alpha}$, where P_0 is constant.

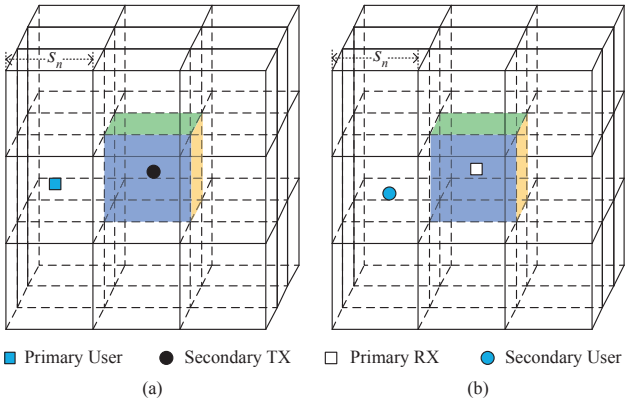

Fig. 4. (a): The interference region of SU, (b): The protected region of PU.

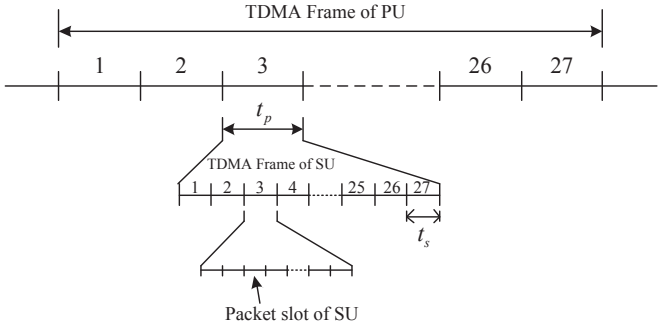

Fig. 5. The frame format of SU, which is an modification of Fig. 4 in [10].

B. Network protocols of SUs

1) The secondary cubes form clusters. Each secondary cluster has 27 secondary cubes. Thus secondary network also adopts 27-TDMA transmission protocol. As illustrated in Fig. 5, the length of secondary frame equals the length of primary time slot. Each frame of SU consists of 27 secondary time slots. Each secondary time slot with time length t_s is allocated to one secondary cube for data transmission. In one cluster, each secondary cube transmits data in a round-robin manner.
2) When a secondary cube is active, it divides its time slot into multiple secondary packet slots. Each routing passing through or originating at the secondary cube uses one of the packet slots to transmit data, which is illustrated in Fig. 5.

3) The data of SU is transmitted from the source to destination following the straight-line routing as illustrated in Fig. 2(a). As in Fig. 2(b), the packets can be transmitted to one of the 6 adjacent cubes.
4) As illustrated in Fig. 4(b), the cluster of 27 secondary cubes with a primary RX at the center cube is the protected region of this PU. When a secondary TX falls into the protected region of this PU, this secondary TX buffers its data and wait for another change to transmit[1].
5) When the distance between a SU and its nearest primary TX is larger than $\frac{s_m}{2}$ and this SU has a transmission time slot, this SU can be active and transmit data[2].
6) The transmit power of SU is $P_1 s_m^{\alpha}$, where P_1 is constant.

C. Connectivity Analysis

When PUs and SUs coexist in the same area, the SUs must be coordinated to mitigate the interference to PUs. The most intuitive way is to deploy low-powered SUs to flexibly exploit the spectrum holes of PUs. As illustrated in Fig. 4(a), the cluster of 27 secondary cubes with a secondary TX at the center cube is the interference region of this SU. Similarly, the cluster of 27 secondary cubes with a primary RX at the center cube is the protected region of this PU, which is illustrated in Fig. 4(b). With some modifications of Lemma 4 in our previous work [13], we have the following lemma.

Lemma 2. *Denote the number of PUs in the interference region of an SU as L, which is a function of n (or m). Then for different values of β, we have three cases as follows.*

1) *If $\beta > 1$, then for any positive number ε,*

$$\lim_{n\to\infty} \Pr\{L \geq \varepsilon\} = 0 \tag{8}$$

namely, L converges to 0 in probability.

2) *If $\beta = 1$, we have*

$$27c_0\left(\frac{1}{2} - \frac{1}{e}\right)\log n \leq L \leq 27c_0 e \log n \tag{9}$$

with high probability (w.h.p.), namely, $L = \Theta(\log n)$.

3) *If $\beta < 1$, we have*

$$27c_0\left(\frac{1}{2} - \frac{1}{e}\right)\log n \leq L \leq 27c_0 e n^{1/\beta - 1}\log n \tag{10}$$

with high probability (w.h.p.).

PUs act as if the SUs do not exist, thus the connectivity of primary network can be guaranteed. According to Lemma 2, the spectrum opportunities exist when $\beta > 1$. Thus we only consider the case $\beta > 1$. As illustrated in Fig. 6, an active primary RX is surrounded by 27 secondary cubes, which form primary protected region. In the primary cluster with 27 primary cubes, this primary protected region can be anywhere. We investigate the SUs in this primary protected region, since these SUs cannot transmit when the primary RX is active. However, these SUs can exploit the transmit slots of the yellow primary cubes. Fig. 6(a) illustrates the worst case, where the active primary RX is located in the intersection of 8 primary cubes. However, in this case, the SUs in this primary protected region can still use 8 primary slots to transmit their own data. If the primary protected region is located within the primary cube, as illustrated in Fig. 6(b)(c)(d), the SUs can exploit 21 primary slots to transmit their own data. Thus with the network protocols of PUs and SUs, each SU has an opportunity to transmit during one primary frame, which consists of 27 primary time slots. Notice that the length of a primary time slot equals to the length of a secondary frame [10], thus the connectivity of secondary network can be guaranteed.

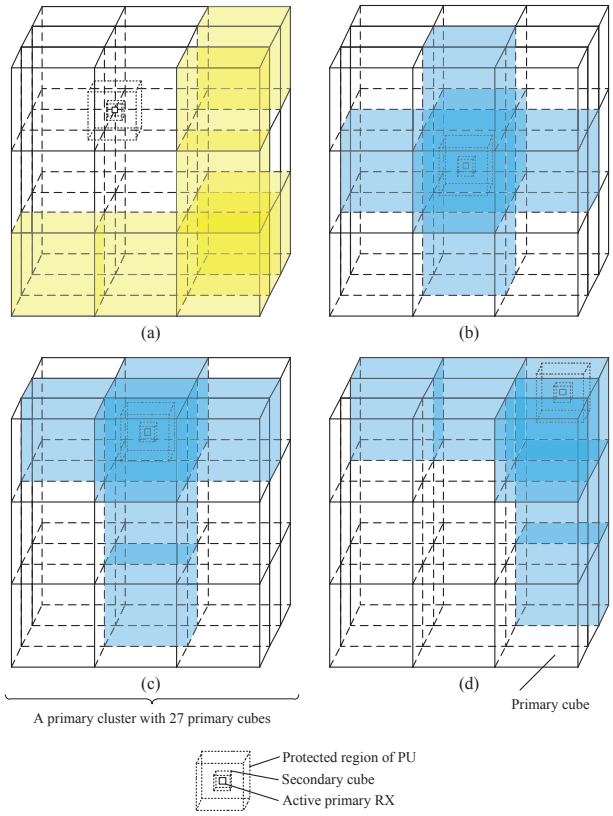

Fig. 6. In a primary cluster with 27 primary cubes, the SUs in the primary protected region can exploit the transmit slots of the yellow primary cubes. However, the SUs in the primary protected region may not use the transmit slots of the blue primary cubes.

D. Capacity of a TX-RX Pair

We investigate the interference suffered by ith primary TX-RX pair, which is derived as follows.

$$\begin{aligned} I_p(i) &= \sum_{k=1,k\neq i}^{m} P_p(k) g(\|X_{p,tx}(k) - X_{p,rx}(i)\|) \\ &< \sum_{t=1}^{\infty} 2(12t^2+1) P_0 s_m^{\alpha} ((3t-2)s_m)^{-\alpha} \\ &= 2P_0 \sum_{t=1}^{\infty} (12t^2+1)(3t-2)^{-\alpha} \end{aligned} \tag{11}$$

[1]When the primary RX at the center cube is inactive, the protected region of this PU disappears.

[2]This operation is to guarantee a nontrivial channel rate of SU.

Similarly, we have

$$I_{sp}(i) < 2P_1 \sum_{t=1}^{\infty} (12t^2+1)(3t-2)^{-\alpha} \tag{12}$$

$$I_s(i) < 2P_1 \sum_{t=1}^{\infty} (12t^2+1)(3t-2)^{-\alpha} \tag{13}$$

$$I_{ps}(i) < 2P_1 \sum_{t=1}^{\infty} (12t^2+1)(3t-2)^{-\alpha} + 2^{\alpha}P_1 \tag{14}$$

We consider an interference dominated environment where noise term in (1) and (2) can be ignored [3]. Notice that the link capacity of a standalone network is derived in [3]. Further, with (11)(12)(13)(14), the link capacity of primary networks and secondary networks can be derived as follows.

Lemma 3. *In the interference dominated environment, the capacity of ith primary TX-RX pair is*

$$R_p(i) \geq \begin{cases} \frac{1}{27}\Theta(m^{\frac{1}{3}(\alpha-3)}) & 2<\alpha<3 \\ \frac{1}{27}\Theta(\frac{1}{\log m}) & \alpha=3 \\ \frac{1}{27}\Theta(1) & \alpha>3 \end{cases} \tag{15}$$

The capacity of the jth secondary TX-RX pair is

$$R_s(j) \geq \begin{cases} \frac{1}{27}\frac{8}{27}\Theta(n^{\frac{1}{3}(\alpha-3)}) & 2<\alpha<3 \\ \frac{1}{27}\frac{8}{27}\Theta(\frac{1}{\log n}) & \alpha=3 \\ \frac{1}{27}\frac{8}{27}\Theta(1) & \alpha>3 \end{cases} \tag{16}$$

where $\frac{1}{27}$ is due to 27-TDMA protocol and $\frac{8}{27}$ is the penalty due to the presence of the preservation region, since in the worst case SU can use 8 primary slots to transmit its own data during a primary frame, which is illustrated in Fig. 6(a).

IV. Achievable Capacity Scaling Laws

Assuming a standalone network with k nodes, we study the situations that a routing generating from X_i passes a cube and have the following lemma.

Lemma 4. *Denote the routing with source X_i and destination Y_i as R_i. For a cube V, we have*

$$\Pr\{R_i \text{ passes } V\} \leq c_1 \left(\frac{\log k}{k}\right)^{2/3} \tag{17}$$

Proof: For cube V, the radius of its circumscribed sphere is $r_k = \frac{\sqrt{3}}{2}(\frac{c_0 \log k}{k})^{1/3}$. As illustrated in Fig. 7, a cone with vertex X_i and height $X_iB = \sqrt{3}$ is constructed. Thus if Y_i falls into the shaded region of Fig. 7, R_i passes V. Because the volume of the total cube is 1, the volume of the shaded region is the probability that R_i passes V, which is upper bounded by $\min\{1, \text{volume of the cone}\}$. The upper bound of the volume of the cone is $\frac{\sqrt{3}\pi r_k^2}{x^2}$. Denote $X = x$ as the distance between X_i and the center of the circumscribed sphere. Because X_i is uniformly distributed, the probability density function of X is $f(x) = c_2 x^2$. Thus we have

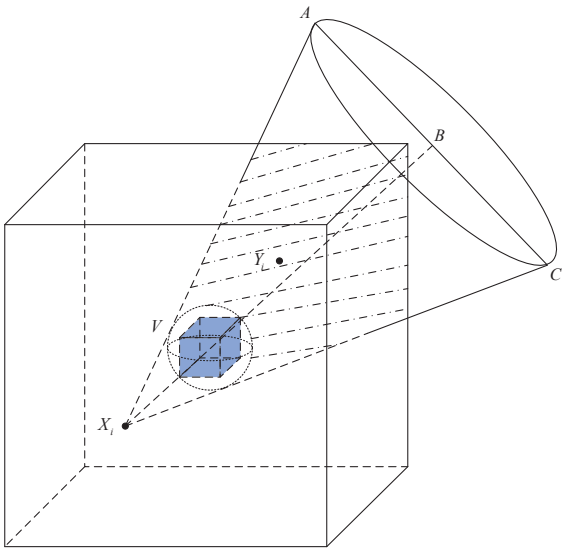

Fig. 7. The situations that a routing passes a cube.

$$\begin{aligned} \Pr\{R_i \text{ passes } V\} &\leq \int_{r_k}^{\sqrt{3}} \min(\frac{\sqrt{3}\pi r_k^2}{x^2}, 1) c_2 x^2 dx \\ &\leq c_1 (\frac{\log k}{k})^{2/3} \end{aligned}$$

■

We derive the number of routings passing through a cube and have the following lemma.

Lemma 5. *Denote the number of routings that pass cube V as M, then M satisfies the following condition.*

$$\lim_{k\to\infty} \Pr\{M > c_3 k^{1/3} (\log k)^{2/3}\} \to 0 \tag{18}$$

where $c_3 > c_1$.

Proof: According to Lemma 4, the probability that a routing passes V is upper bounded by $c_1(\frac{\log k}{k})^{2/3} \triangleq p$. Define an indicator $I_i = 1$ representing that ith routing passes V and otherwise $I_i = 0$. Thus the number of routings passing V is $Z_k = \sum_{i=1}^{k} I_i$. The Chernoff inequality is used to obtain the upper bound of Z_k. For any positive number a, x, we have

$$\Pr\{Z_k > x\} \leq \frac{E\left[\exp\left(aZ_k\right)\right]}{\exp\left(ax\right)} \tag{19}$$

And we have

$$\begin{aligned} E\left[\exp\left(aZ_k\right)\right] &= \left(1+(e^a-1)p\right)^k \leq \exp\left(k(e^a-1)p\right) \\ &\leq \exp(c_1(e^a-1)k^{1/3}(\log k)^{2/3}) \end{aligned} \tag{20}$$

Substitute $x = c_3 k^{1/3}(\log k)^{2/3}$ into (19), we have

$$\begin{aligned} &\Pr\{Z_k > c_3 k^{2/3}(\log k)^{1/3}\} \\ &\leq \exp\left(\left(c_1(e^a-1)-c_3\right)k^{1/3}(\log k)^{2/3}\right) \end{aligned} \tag{21}$$

If $c_3 > c_1$, an appropriate positive number a can be chosen such that when $k \to \infty$, $\Pr\{Z_k > c_3 k^{2/3} (\log k)^{1/3}\} \to 0$. Now we need to prove that for any cube, the number of routings passing this cube, which is denoted as $Z_{cube,k}$, would not exceed $c_3 k^{2/3} (\log k)^{1/3}$ with high probability.

$$\begin{aligned} &\Pr\{Z_{cube,k} > c_3 k^{2/3} (\log k)^{1/3}\} \\ &\overset{(a)}{\leq} \frac{1}{s_k^3} \exp\left(\left(c_1 (e^a - 1) - c_3\right) k^{1/3} (\log k)^{2/3} \right) \to 0 \end{aligned} \tag{22}$$

where (a) is achieved using the union bound. Therefore Lemma 5 is proved. ∎

Because the PUs act as if the SUs do not exist, thus the capacity of primary network is the same as the capacity of standalone network with the same number of nodes. In Lemma 3, we have achieved the capacity of the ith primary TX-RX pair, which is the capacity that a primary cube can support. In Lemma 5, we have derived the maximum number of routings that pass a primary cube[3]. Thus the achievable per-node capacity can be derived as the capacity of primary TX-RX pair divided by the number of routings that pass a primary cube [14], which is presented as follows.

Theorem 1. *In the interference dominated environment, the achievable per-node capacity of primary network is*

$$\lambda_p(m) \geq \begin{cases} \Theta(\frac{1}{m^{4/3-\alpha/3} (\log m)^{2/3}}) & 2 < \alpha < 3 \\ \Theta(\frac{1}{m^{1/3} (\log m)^{5/3}}) & \alpha = 3 \\ \Theta(\frac{1}{m^{1/3} (\log m)^{2/3}}) & \alpha > 3 \end{cases} \tag{23}$$

With the network protocols in this paper, the connectivity of SUs can be guaranteed. As illustrated in Fig. 6, due to the presence of primary protected region, each SU can at least use $\frac{8}{27}$ of primary slots to transmit its own data, which is finite and would not change the capacity scaling laws. Thus the capacity scaling laws of secondary networks can be similarly derived.

Theorem 2. *In the interference dominated environment, the achievable per-node capacity of secondary network is*

$$\lambda_s(n) \geq \begin{cases} \Theta(\frac{1}{n^{4/3-\alpha/3} (\log n)^{2/3}}) & 2 < \alpha < 3 \\ \Theta(\frac{1}{n^{1/3} (\log n)^{5/3}}) & \alpha = 3 \\ \Theta(\frac{1}{n^{1/3} (\log n)^{2/3}}) & \alpha > 3 \end{cases} \tag{24}$$

Notice that the achievable capacity of 2D cognitive radio networks is $\Theta(\frac{1}{\sqrt{n \log n}})$. Therefore when $\alpha > 2.5$, the capacity of 3D cognitive radio networks is superior to 2D cognitive radio networks with the same number of nodes asymptotically.

V. Conclusion

In this paper, we have analyzed the capacity scaling laws of 3D cognitive radio networks. Firstly, we design the network protocols to coordinate the interference and guarantee the connectivity of primary network and secondary network. Then we investigate the capacity of a TX-RX pair and the number of routings in a primary and secondary cube. Finally, we have derived the per-node capacity of primary network and secondary network respectively. We have verified that the path loss factor α has an impact on the capacity of 3D CRNs, namely, $\alpha = 3$ is a watershed of capacity scaling laws. Besides, when $\alpha > 2.5$, the capacity of 3D CRNs is higher than 2D CRNs with the same amount of nodes asymptotically. Since the modern wireless networks will be widely deployed in the 3D space, our results may provide an insight into the network design and performance analysis of three dimensional cognitive radio networks.

[3]We only need to substitute $k = m$ in Lemma 5

Acknowledgment

The authors thank Prof. Changchuan Yin for the helpful advices. This work was supported by the National Natural Science Foundation of China (61525101,61227801), the National High-Tech R&D Program (863 Program) under grant No. 2015AA01A705, the National Key Technology R&D Program of China (2015ZX03002008-002).

References

[1] S. Haykin, "Cognitive Radio: Brain-Empowered Wireless Communications," IEEE Journal on Selected Areas in Communications, vol. 23, no. 2, pp. 201-220, Feb. 2005.

[2] T. Yucek and H. Arslan, "A survey of spectrum sensing algorithms for cognitive radio applications," IEEE Communications Surveys & Tutorials, vol. 11, no. 1, pp. 116-130, Mar. 2009.

[3] P. Li, M. Pan, and Y. Fang, "Capacity bounds of three-dimensional wireless ad hoc networks," IEEE/ACM Transactions on Networking, vol. 20, no. 4, pp. 1304C1315, 2012.

[4] P. Gupta and P. R. Kumar, "The capacity of wireless networks," IEEE Transactions on Information Theory, vol. 46, no. 2, pp. 388-404, Mar. 2000.

[5] P. Gupta, P. R. Kumar et al., "Internets in the sky: The capacity of three dimensional wireless networks," Communications in Information and Systems, vol. 1, no. 1, pp. 33C49, 2001.

[6] C. Hu, X. Wang, Z. Yang, J. Zhang, Y. Xu, X. Gao, "A Geometry Study on the Capacity of Wireless Networks via Percolation," IEEE Transactions on Communications, vol. 58, no. 10, pp. 2916-2925, Oct. 2010.

[7] G. Bai, L. Yu, Q. Liu, "An Achievable Throughput Capacity of Three-Dimensional Inhomogeneous Wireless Networks," IEEE 80th Vehicular Technology Conference (VTC Fall), pp. 1-5, Sep. 2014.

[8] S.-W. Jeon, N. Devroye, M. Vu, S.-Y. Chung, and V. Tarokh, "Cognitive networks achieve throughput scaling of a homogeneous network," IEEE Transactions on Information Theory, vol. 57, no. 8, pp. 5103-5115, Aug. 2011.

[9] S.-W. Jeon, M. Gastpar, "Capacity Scaling of Cognitive Networks: Beyond Interference-Limited Communication" IEEE Transactions on Information Theory, vol. 60, no. 12, pp. 7824 - 7840, Dec. 2014.

[10] C. Yin, L. Gao and S. Cui, "Scaling Laws for Overlaid Wireless Networks: A Cognitive Radio Network versus a Primary Network," IEEE/ACM Transactions on Networking, vol. 18, no. 4, pp. 1317-1329, Aug. 2010.

[11] C. Wang, C. Jiang, S. Tang, X. -Y. Li, "Scaling Laws of Cognitive Ad Hoc Networks over General Primary Network Models" IEEE Transactions on Parallel and Distributed Systems, vol. 24, no. 5, pp. 1030 - 1041, May 2013.

[12] C. Wang, S. Tang, X.-Y. Li, C. Jiang, "Multicast Capacity Scaling Laws for Multihop Cognitive Networks" IEEE Transactions on Mobile Computing, vol. 11, no. 11, Nov. 2012.

[13] Z. Wei, Z. Feng, Q. Zhang, W. Li and T. A. Gulliver, "Throughput scaling laws of cognitive radio networks with directional transmission," IEEE Global Communications Conference (GLOBECOM), pp. 872-877, Dec. 2013.

[14] X. Feng and P. R. Kumar, "Scaling laws for ad hoc wireless networks: An information theoretic approach," Foundations and Trends in Networking, vol. 1, no. 2, pp. 145-270, 2006.

[15] P. Li, M. Pan, and Y. Fang, "The capacity of three-dimensional wireless ad hoc networks," IEEE International Conference on Computer Communications (INFOCOM), pp. 1485 - 1493, Apr. 2011.